

Thermoreversible gelation of poly[hexyl isocyanate]: Effect of solvent type

Sandrine Poux^{a,1}, Sudip Malik^a, Annette Thierry^a, Marcel Dosiere^b, Jean-Michel Guenet^{a,b,*}

^a Institut Charles Sadron, CNRS UPR 22, 6 rue Boussingault, BP 40016, F-67083 Strasbourg Cedex, France

^b Laboratoire de Physico-chimie des Polymères, Université de Mons-Hainault, Place du Parc, 20 B-7000 Mons, Belgium

Received 14 February 2005; received in revised form 10 September 2005; accepted 13 September 2005

Available online 11 May 2006

Abstract

The thermoreversible gelation of poly[hexyl isocyanate] (PHIC), a rather stiff polymer, has been studied in two closely-related solvents of the alkane series, namely heptane and octane. Temperature–concentrations phase diagrams have been established for both systems. The occurrence of polymer–solvent compound is suggested in heptane but not in octane. This conclusion receives further support from neutron diffraction investigations through the use of the isotopic labelling technique. Finally, it is observed that the morphology is also affected by the solvent type although still displaying a fibrillar network structure.

© 2006 Elsevier Ltd. All rights reserved.

Keywords: Thermoreversible gelation; Phase diagrams; Polymer solvent compounds

1. Introduction

A large variety of synthetic polymers can form thermo-reversible gels of fibrillar morphology that arises from the intrinsic stiffness of the chains or from the enhancement of chain persistence length through mechanisms such as helix stabilization by solvation [1,2]. As chain-folding is eventually hampered chains organization can only occur through bunching thus giving birth to fibrils instead of spherulites. This clearly promotes the formation of the fibrillar morphology of this class of thermoreversible gels [3,4].

Poly[*n*-hexyl isocyanate] (PHIC), belongs to the category of stiff polymers [5,6]. Liquid crystalline mesophases can be observed at high polymer concentrations, as well as fibrillar gels at moderate polymer concentrations [6–9]. In principle, due to the intrinsic stiffness of PHIC chains, the solvent type should not play the same role as that reported for isotactic polystyrene [2]. In the latter case, the enhancement of chain persistence length is due to the stabilization of the helical structure by the solvent whose size is thereby an important

parameter [10]. Yet, it will be shown in this paper that gels differ significantly whether one uses two very closely-related solvents, namely heptane and octane. Temperature–concentration phase diagrams, X-ray and neutron diffraction, and morphology investigations presented in this paper will highlight these differences.

2. Experimental

2.1. Materials

The poly[hexyl isocyanate] sample used in this study was synthesized by means of a process devised by scientists from Dupont [11] and was purchased from Polysciences. The weight-average molecular weight was found to be: $M_w = 8 \times 10^4$ g/mol with $M_w/M_n = 1.44$ [5,12]. The solvents octane and heptane were purchased from Aldrich and were used without further purification. Deuterated solvents were from the same company, and were also used without further purification.

2.2. Techniques and sample preparation

The gel thermal behaviour was investigated by means of a DSC 7 from Perkin–Elmer operating at different heating and cooling rates. For concentrations below 30% (w/w) in octane or in heptane, homogeneous solutions were first prepared in closed test tubes. Cooling these solutions to room temperature produced a gel, a piece of which, approximately 30 mg, was

* Corresponding author. Address: Institut Charles Sadron, CNRS UPR 22, 6 rue Boussingault, BP 40016, F-67083 Strasbourg Cedex, France. Tel.: +33 388 41 40 00; fax: +33 388 41 40 99.

E-mail address: guenet@ics.u-strasbg.fr (J.-M. Guenet).

¹ Present address: Universität Basel, Abteilung Chemie, Klingelbergstrasse, 80, CH-4056 Basel, Switzerland.

rapidly transferred into stainless steel pans that were hermetically sealed. For higher concentrations, samples were obtained by prior evaporation of the solvent from pieces of gel of concentrations below 30%. For all the systems obtained from less concentrated solutions, heating and annealing close to the solvent boiling point were first performed inside the DSC pan to obtain homogeneous sample. After each cycle (cooling–heating–cooling) the weight loss was systematically measured.

The temperature–concentration phase diagrams were established after extrapolation to zero heating rate of the temperatures corresponding to the different melting events.

Scanning Electron Microscopy (SEM) investigations were performed on gels dried at room temperature while left on their glass or silicon supports. A conducting 80 nm thick coating gold layer was deposited by sputtering in an argon atmosphere. The observation of the surface topography was performed with a Hitachi S-2300 microscope operating at voltages ranging from 15 to 25 kV.

The X-ray diffraction measurements were performed at Mons-Hainaut University on a RIGAKU RU200 device equipped with a point focus rotating anode from which a Ni-filtered Cu K $_{\alpha}$ radiation was delivered ($\lambda=0.1542$ nm). The intensities were recorded on square image plates with an area of about 140 cm 2 and were scanned with 50 μ m resolution on a FUJI X BAS-3000 image analyser. The data were analysed using an X-ray software developed at Mons University (search of the beam centre, Lorentz and polarization corrections, determination of the intensity profile as a function of the scattering angle). Energy minimization for determining the helical structure and calculation of the diffraction patterns were carried out by using Cerius 42 software from Accelrys.

The samples were prepared by introducing in Lindenmann glass capillaries of 2 mm diameter pieces of gels prepared beforehand in test tubes. Capillaries were eventually sealed from atmosphere.

Neutron diffraction experiments were carried out on D16 camera located at ILL (Institut Laue Langevin, Grenoble, France). D16 is a two-circle diffractometer with a focusing monochromator consisting of nine vertical bending pyrolytic graphite (002) crystals. By operating at two neutron wavelengths (0.45 and 0.56 nm, with $\Delta\lambda/\lambda \approx 1\%$) the resulting momentum transfer is in the range $0.5 < q < 24$ nm $^{-1}$ with momentum transfer resolution $q=0.035$ nm $^{-1}$. Neutrons are counted by means of a position-sensitive gas multidetector (with 128×128 wires) that can be scanned around the sample to observe diffraction out to an angle of about 120°. (further details available at the following website: http://www.ill.fr/pages/science/IGroups/sc_frst_2.html).

The samples were prepared in hermetically-sealed quartz cells from HELIMA into which the desired quantity of each constituent was introduced beforehand. The mixture were heated at 130 °C until a clear, homogeneous solution was obtained, and then quenched to room temperature so as to form the gel.

3. Results and discussion

3.1. Thermodynamics: temperature–concentration phase diagram

Typical thermograms obtained on cooling and on heating (in both case at a rate of 10 °C/mn) are drawn in Fig. 1 for the system PHIC/heptane for different polymer concentrations. As can be seen, two endotherms on cooling and on heating are observed for concentrations above 5%. The temperatures recorded on heating that are associated with all the first order events are reported in Fig. 2 in order to establish the temperature–concentration phase diagram. In the same figure are also plotted the values of the latent heats associated with the same first order events as a function of concentration (Tamman's diagram). These enthalpies are obtained by performing a deconvolution of the two-peak endotherms as shown in Fig. 1. Also, the melting enthalpy of the solvent, that has been crystallized after gelation of the polymer, is plotted on the same diagram. When the melting enthalpy of the solvent becomes zero at concentration C_{γ} one obtains a measure of the fraction of solvent trapped in the polymer through [13]

$$\alpha = \frac{1 - C_{\gamma}}{C_{\gamma}} \times \frac{m_p}{m_s} \quad (1)$$

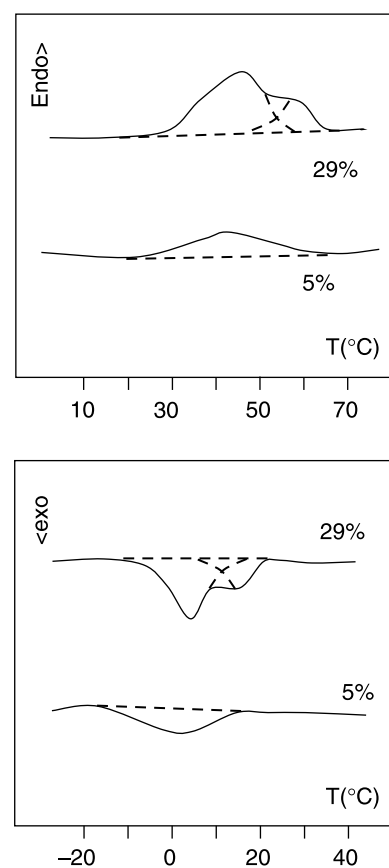


Fig. 1. Typical DSC traces obtained on heating and on cooling PHIC/heptane gels at 10 °C/min. Peak deconvolution is shown. Concentrations in g/g as indicated. Bottom, cooling; Top, heating.

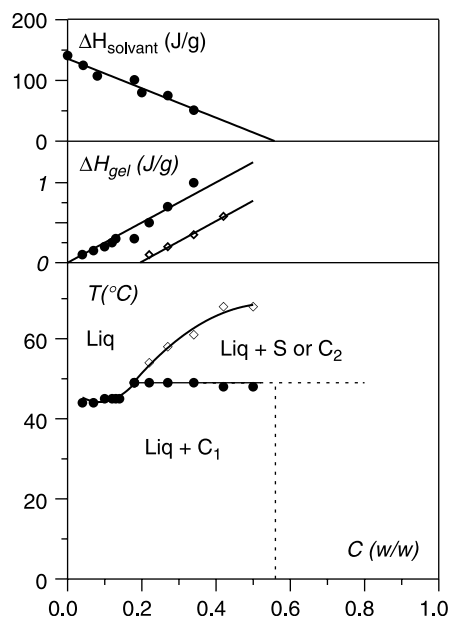


Fig. 2. Bottom: temperature–concentration phase diagram for the system PHIC/heptane. As is customary, the full lines represent known transitions while dotted lines represent probable extensions. Middle: enthalpy associated with various thermal events. (●)=incongruent melting (◇)=terminal melting. Top: melting enthalpy of the free solvent as a function of polymer concentration.

where α is the number of solvent molecules per monomer unit, m_p and m_s the molecular weight of the polymer and of the solvent, respectively. In the present case, the value of the parameter α is $\alpha = 1.27 \pm 0.15$ solvent molecules/monomer unit. As will be discussed in what follows a large fraction of the solvent is trapped because it forms a compound with the polymer (polymer–solvent compound). The shape of the phase diagram, and particularly the non-variant event occurring at $T = 49 \pm 2$ °C, is consistent with the existence of such a polymer–solvent compound [14,15]. This non-variant event could correspond to a desolvation transition, or in other words to an incongruent-melting process of the type:

compound \Rightarrow solid + solvent

Higher concentrations needed to determine with accuracy the stoichiometric composition could not be explored because of the lack of reproducibility. This most probably arises from the fact that the solutions become very viscous, which prevents from preparing homogeneous samples. At any rate the stoichiometry composition cannot exceed the value of α . For a fraction of organized polymer close to 100% α is equal to the stoichiometry. If this fraction is lower than 100%, which is certainly the case here, and also if the amorphous domains are more solvated than the organized domains, then the stoichiometry should be significantly lower than α .

This can be demonstrated through the following equation

$$\left(\frac{n_s^c}{n_m^c}\right) = \frac{1 - C_\gamma [1 + (1 - X_c)(n_s^a/n_m^a)(m_s/m_p)]}{X_c C_\gamma} \times \frac{m_p}{m_s} \quad (2)$$

where X_c is the crystallinity, (n_s^c/n_m^c) for the number of solvent molecules per monomer in the compound phase (namely the real value of the compound stoichiometry), and (n_s^a/n_m^a) the number of solvent molecules per monomer in the amorphous phase.

If $X_c = 1$ or $(n_s^a/n_m^a) = (n_s^c/n_m^c)$, one then retrieves relation (1). If the amorphous phase is more solvated than the compound, then the apparent stoichiometry derived from (1) to be larger than the actual value calculated from relation (2). Presently, we do not know the degree of solvation in the amorphous phase nor the exact crystallinity so that the real stoichiometry cannot be derived.

Typical DSC traces obtained at different polymer concentration are reported on Fig. 3 for the system PHIC/octane. As can be seen only one endotherm can be observed unlike what occurs for PHIC/heptane. The temperature–concentration phase diagram is drawn in Fig. 4. Clearly, this phase diagram differs from that obtained with PHIC/heptane systems as no non-variant event is seen. In addition, the value of α determined from solvent crystallization is now $\alpha = 0.15 \pm 0.04$. This very low value, together with the absence of a non-variant event, implies a polymer organization without solvent, namely no polymer–solvent compound is formed. Note that in the case of a 100% organized polymer the value of α should be zero if no solvent were occluded. That it slightly differs from zero probably arises from the presence of a low content of solvent molecules that are trapped within the amorphous

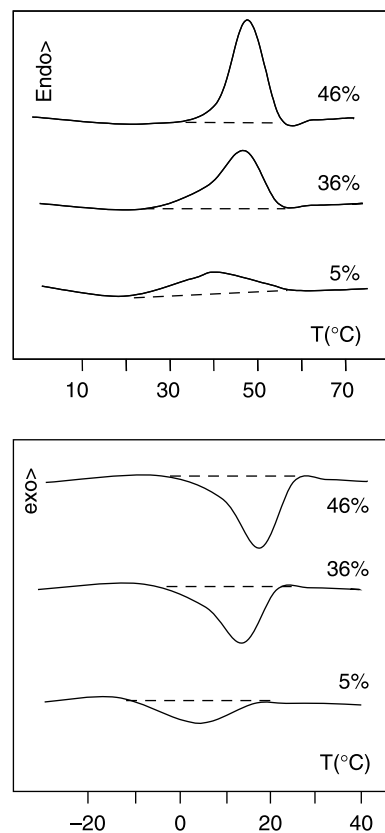


Fig. 3. Typical DSC traces obtained on heating and on cooling PHIC/octane gels at 10 °C/min. Concentrations in g/g as indicated. Bottom, cooling; Top, heating.

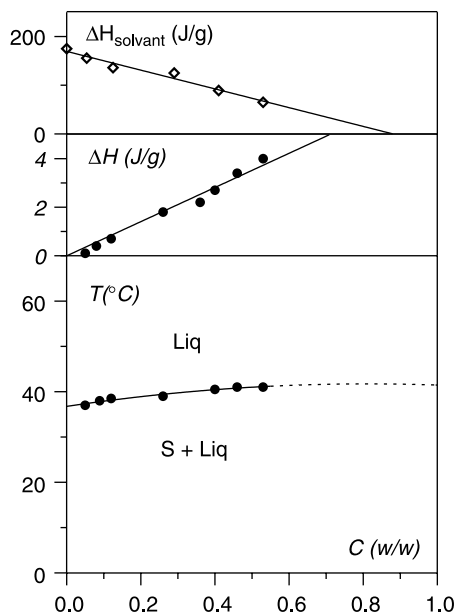


Fig. 4. Bottom: temperature–concentration phase diagram for the system PHIC/octane. As is customary, the full lines represent known transitions while dotted lines represent probable extensions. Middle: enthalpy associated with the gel melting. Top: melting enthalpy of the free solvent for the system PHIC/octane as a function of polymer concentration.

domains. Also, worth noting is the occurrence of lower melting temperatures together with larger melting enthalpies in PHIC/octane systems with respect to PHIC/heptane systems. This implies that the melting entropy ΔS_m ($\Delta S_m = \Delta H_m/T_m$) is markedly different in each system, namely $\Delta S_m^{\text{hep}} < \Delta S_m^{\text{oct}}$. This most probably arises from the presence or absence of solvent molecules in the organized state as the variation of entropy when melting is expected to be lower for solvated systems in terms of the number of possible conformational states.

3.2. Molecular structure by diffraction techniques

The crystalline structure has been studied by X-ray and neutron diffraction. In Fig. 5 are plotted the X-ray diffraction patterns obtained both with PHIC/octane and PHIC/heptane systems at a polymer concentration of $C=0.3$ w/w. As is apparent from this figure, the positions of the reflections are not system-dependant, only the intensity of the first reflection turns out to be higher for PHIC/octane systems. Table 1 summarizes the distances associated with the observed reflections as derived from Bragg's law [16].

The existence of a polymer–solvent complex can be further confirmed by neutron diffraction through the use of the isotopic labelling [17,18]. As a matter of fact, the diffracted intensity can be written in a very general way

$$I(q) \propto K_p^2 S_p(q) + K_s^2 S_s(q) + 2K_p K_s S_{ps}(q) \quad (3)$$

in which K and $S(q)$ are, with the appropriate subscripts, the contrast factor and the structure factor of the polymer and the solvent, and $S_{ps}(q)$ is a cross-term which is relevant in the case of polymer–solvent compounds. In the absence of such

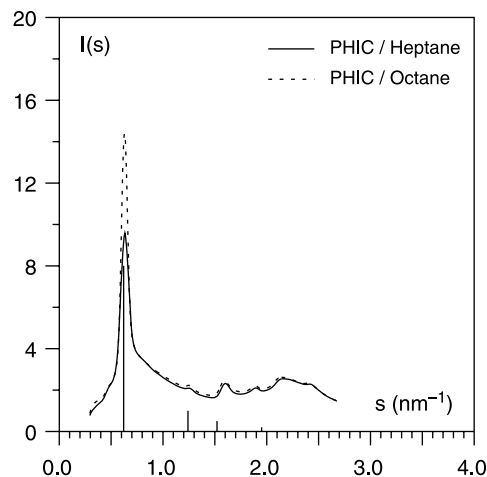


Fig. 5. X-ray diffraction pattern for $C=0.3$ w/w gels in heptane (full line) and in octane (dashed line). $s=2\sin(\theta/2)/\lambda$ where λ is the X-ray wavelength (0.154 nm) and θ is the diffraction angle. The bold vertical lines stand for the position of the reflection together with their relative intensities as calculated with a orthorhombic unit cell with parameters $a=b=1.66$ nm, $\gamma=104^\circ$ and $c=1.54$ nm.

a compound relation (1) reduces to:

$$I(q) \propto K_p^2 S_p(q) + K_s^2 S_s(q) \quad (4)$$

As the solvent is a liquid at room temperature, the second term in relation (4) will not contribute to the crystalline diffraction, but only give a halo. Changing the contrast factor of the solvent, by using deuterated instead of hydrogenous solvent will therefore have not effect on the polymer diffraction pattern, and correspondingly on the entire diffraction pattern [17,18]. Conversely, due to the existence of a cross-term $S_{ps}(q)$ in relation (3), the diffraction pattern of the polymer–solvent compound will depend strongly on the isotopic labelling of the solvent.

As shown in Fig. 6, diffracted intensities are strongly affected in the case of PHIC/heptane systems unlike what is seen with PHIC/octane systems. The diffraction experiments have been carried out under the same conditions of concentration and temperature. In the case of PHIC/octane, the intensities (peak area) are virtually identical whether deuterated or hydrogenous solvent is used. In the case of PHIC/heptane, the intensity is about three times larger when using deuterated instead of hydrogenous heptane. Also, the appearance of a second peak thanks to solvent labelling for PHIC/heptaneD while this is not the case for PHIC/octaneD, gives further support to the

Table 1
Distances associated with the different reflections observed by X-ray diffraction

No	d (nm)	Intensity
1	1.61	vs
2	0.79	m
3	0.62	s
4	0.52	m
5	0.46	w
6	0.41	w

vs, very strong; s, strong; m, medium; w, weak.

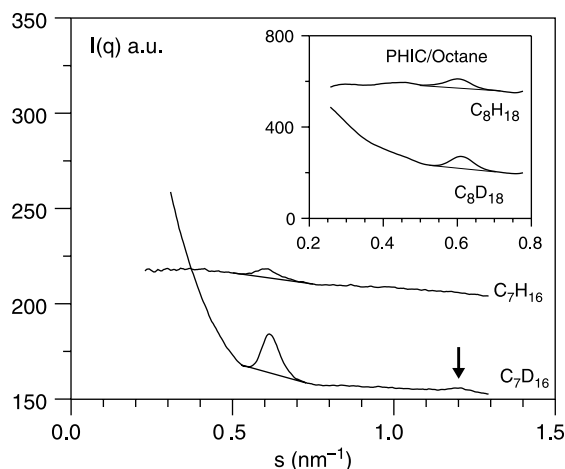


Fig. 6. Neutron diffraction patterns for $C=0.3$ w/w gels in heptane: top: deuterated poly[hexyl isocyanate] in hydrogenous heptane; bottom: deuterated poly[hexyl isocyanate] in deuterated heptane. Arrow indicates the appearance of a second peak due to solvent labelling. Inset: neutron diffraction pattern for $C=0.3$ w/w gels in octane: top: deuterated poly[hexyl isocyanate] in hydrogenous octane; bottom: deuterated poly[hexyl isocyanate] in deuterated octane. $s=2 \sin(\theta/2)/\lambda$ where λ is the neutrons wavelength (0.45 nm) and θ is the diffraction angle.

existence of a PHIC/heptane compound. These results bear out the conclusions drawn from the phase diagram. Note that the observation of a more intense first reflection in X-ray diffraction may originate from the same type of contrast effect.

The data gathered in Table 1 clearly indicate that a pseudo-hexagonal lattice as that considered for poly[butyl isocyanate] by Schmueli et al. [16] is not appropriate, although PHIC is said to adopt also a 8_3 helical structure. As a matter of fact, one should observe a reflection at $s=0.71 \text{ nm}^{-1}$ ($d=1.41 \text{ nm}$) with Schmueli et al.'s lattice, which is conspicuously absent both in the X-ray and the neutron diffraction patterns. With the data at hand it is difficult to work out the crystal lattice for poly[hexyl isocyanate], and only a tentative lattice can be proposed for which the reflection at $s=0.71 \text{ nm}^{-1}$ is absent. Under these conditions a orthorhombic unit cell (Fig. 7) with $a=b=1.66$, $c=1.54 \text{ nm}$ and $\gamma=104^\circ$ can reproduce the position of the observed reflections (Fig. 5). This lattice possesses a density of about 0.82 g/cm^3 , and also displays channels that can certainly house solvent molecules. Needless to mention that additional experiments are required, particularly on oriented samples, to determine with a better accuracy the actual crystalline lattice.

3.3. Morphology

Unlike the case of some polymer producing chain-folded crystals, where special preparation techniques for electron microscopy investigations such as that devised by Olley and Bassett [19] have to be used, fibrillar gels can be observed by scanning electron microscopy just after being dried. To be sure, drying may introduce some alterations to the sample although the original morphology is often well preserved. Typical electron micrographs are shown in Fig. 8 for systems prepared at $C=0.3$ w/w in either solvents. As is apparent from these

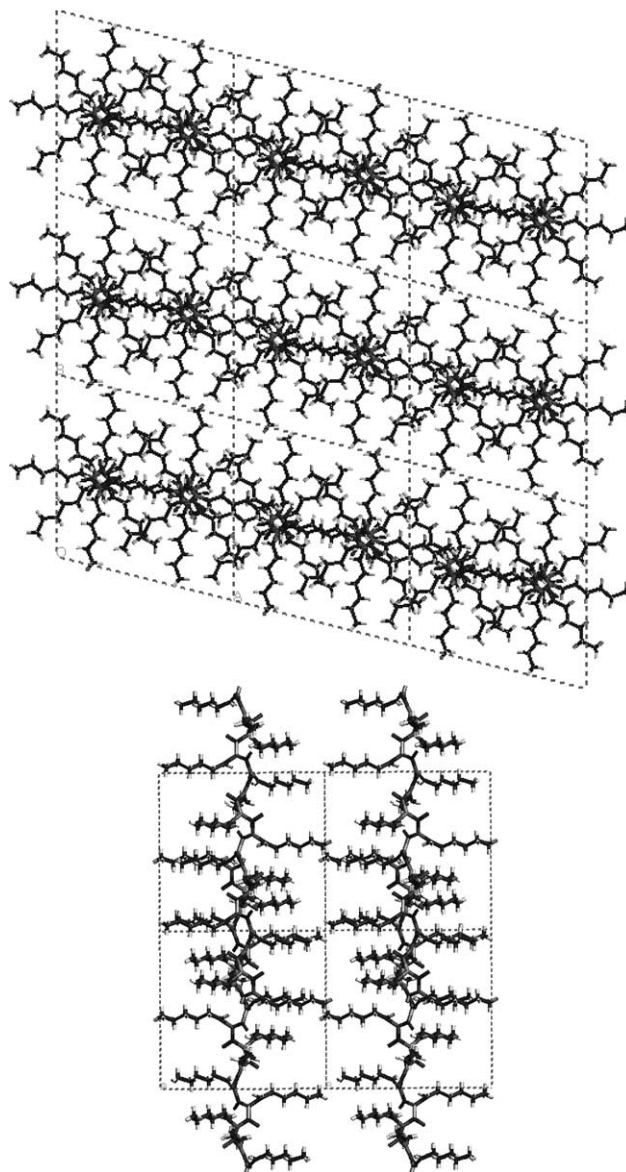


Fig. 7. A possible lattice for PHIC systems (orthorhombic). Upper figure = lattice as seen parallel to the helix axis, lower = lattice as seen perpendicular to the helix axis. $a=b=1.66 \text{ nm}$, $\gamma=104^\circ$ and $c=1.54 \text{ nm}$ (a 8_3 helix is considered).

figures, although both morphologies display a network structure, the fibrils constituting this network have differing structures. The fibrils cross section in PHIC/heptane systems looks rather rectangular while that of PHIC/octane systems appears more cylindrical. Possibly, this morphological difference lies in the fact that solvated crystals are dealt with in the case of PHIC/heptane systems as opposed to PHIC/octane systems.

4. Concluding remarks

Results presented here show that a slight change of solvent structure has a dramatic effect on the thermodynamic properties, but also on the morphology while the crystalline structure is little affected. The occurrence of a compound with heptane as opposed to a solid solution with octane originates possibly in

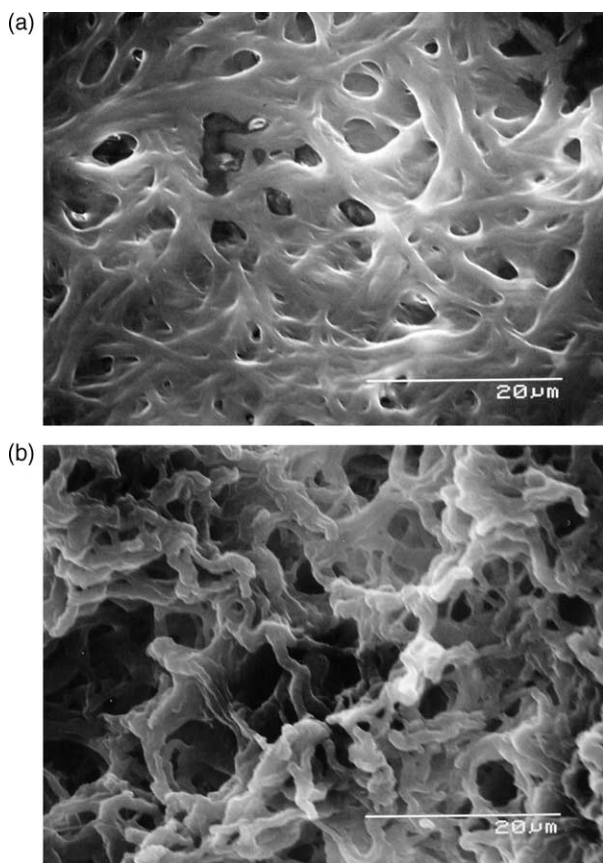


Fig. 8. Scanning electron micrographs obtained after solvent extraction: (a) PHIC/heptane gels $C=0.3$ w/w, (b) PHIC/octane gels $C=0.3$ w/w. Scale as indicated.

the large channels with the crystalline lattice. These channels probably exist because of the peculiar structure of PHIC, namely its long aliphatic side groups. Compound formation then possibly result from a better affinity of PHIC towards heptane than octane. Clearly, compound formation is a consequence of the crystalline lattice, which is capable of housing or not solvent molecules, and not the reverse situation. In this sense PHIC differs from polymers such as syndiotactic

polystyrene for which the non-solvated crystal form differs conspicuously from the solvated one.

Acknowledgements

The X-ray diffraction experiments presented here were carried out as part of a Professorship granted to J.M. Guenet by the FNRS (Fond National de la Recherche Scientifique, Belgium) at Mons-Hainaut University for the academic year 2003–2004. The authors are indebted to C. Straupé and S. Zehnacker for SEM and DSC investigations, respectively.

References

- [1] Guenet JM. Thermoreversible gelation of polymers and biopolymers. London: Academic Press; 1992.
- [2] Guenet JM. Trends Polym Sci 1996;4:6.
- [3] Miller WG, Kou L, Tohyama K, Voltaggio V. J Polym Sci Polym Symp 1978;65:91.
- [4] Guenet JM, Jeon HS, Khatri C, Jha SK, Balsara NP, Green MM, et al. Macromolecules 1997;30:4590.
- [5] Murakami H, Norisuye T, Fujita H. Macromolecules 1980;13:345.
- [6] Green MM, Peterson NC, Sato T, Teramoto A, Lifson S. Science 1995; 268:1860.
- [7] Green MM, Khatri CA, Reidy MP, Levon K. Macromolecules 1993;26: 4723.
- [8] Olayo H, Miller WG. J Polym Sci Polym Phys 1991;29:1473. Turunen T, Tenhu T, Samarianov B, Timofeev VP. Polymer 1995;36:4097.
- [9] Green MM, Reidy MP, Johnson RD, Darling D, O'Leary DJ, Willson G. J Am Chem Soc 1989;111:6452.
- [10] Klein M, Brûlet A, Guenet JM. Macromolecules 1990;23:540.
- [11] Shashoua VE, Sweeney W, Tietz RF. J Am Chem Soc 1960;82:866.
- [12] Ito T, Chikiri H, Teramoto A, Aharoni SM. Polym J 1988;20:143.
- [13] Klein M, Guenet JM. Macromolecules 1989;22:3716.
- [14] See for instance Carbonnel L, Guieu R, Rosso JC. Bull Soc Chim 1970;8– 9:2855. Rosso JC, Guieu R, Ponge C, Carbonnel L. Bull Soc Chim 1973; 9–10:2780.
- [15] Reisman A. Phase equilibria. New York: Academic Press; 1970.
- [16] Shmueli U, Traub W, Rosenheck K. J Polym Sci, Part A2 1969;7:515.
- [17] Point JJ, Damman P, Guenet JM. Polym Commun 1991;32:477.
- [18] Daniel C, DeLuca MD, Brûlet A, Menelle A, Guenet JM. Polymer 1996; 37:1273.
- [19] Olley RH, Bassett DC. Polymer 1982;23:1707.